Investigation of swelling pressure of bentonite/claystone mixture in the full range of bentonite fraction

Zhixiong Zeng[1], Yu-Jun Cui[1], Feng Zhang[1], Nathalie Conil[2], Jean Talandier[2]

1: Ecole des Ponts ParisTech, Laboratoire Navier/CERMES, 6 et 8 avenue Blaise Pascal, 77455 Marne La Vallée cedex 2, France
2: CMHM, Andra, RD 960, 55290 Bure, France

Corresponding author

Professor Yu-Jun Cui

Ecole des Ponts ParisTech, Laboratoire Navier/CERMES, 6 – 8 av. Blaise Pascal, Cité Descartes, Champs-sur-Marne, 77455 Marne – la – Vallée cedex 2, France
Tel.: +33 164153550
Fax: +33 164153562

E-mail address: yu-jun.cui@enpc.fr

Abstract: MX80 bentonite/Callovo-Oxfordian (COx) claystone mixture has been proposed as a sealing/backfilling material in a deep geological repository of radioactive waste in France. A good understanding of the swelling behaviour of this mixture is essential when evaluating the long-term performance of the repository. In this work, the swelling pressure of MX80 bentonite/COx claystone mixture was investigated by the constant-volume method for a full range of bentonite fraction. Results show that the swelling of claystone in the mixture can be inhibited by bentonite and its contribution to the global swelling pressure depends on the bentonite fraction. For the mixture with more than 70% bentonite, claystone behaves as an inert material, and its contribution to the global swelling pressure can be ignored. However, for the mixture with less bentonite, the swelling of claystone will significantly contribute to the global swelling pressure. A method was proposed allowing the swelling pressure of bentonite/claystone mixture to be predicted in the full range of bentonite fraction.

Keywords: bentonite/claystone mixture; swelling pressure; bentonite dry density; inhibition effect; prediction method

1 Introduction

Deep geological disposal has been adopted for radioactive waste in many countries such as China, Belgium, France, Germany, Japan, Sweden, etc. (Gray et al., 1984; Dixon et al., 1985; Sellin and Leupin, 2013). To ensure the isolation of radioactive waste from the surrounding environment, bentonite-based materials are often considered as possible sealing/backfilling materials because of their favorable swelling characteristics and low permeability (Pusch, 1982; Dixon et al., 1985; Komine and Ogata, 1994, 1999; Villar and Lloret, 2008). Once the disposal galleries are closed, pore water from the host rock will progressively infiltrate into the sealing/backfilling materials. They will swell and seal the technological voids between the blocks of compacted bentonite-based materials or between the blocks and the canisters/the host rock (Bian et al., 2018). Afterwards, swelling pressure will develop (Pusch, 1982; Wang et al., 2012). This swelling pressure must be high enough to ensure the good sealing performance, but lower than the in situ minor stress in the host rock (Saba et al., 2014). Therefore, the swelling pressure of bentonite-based materials becomes a key factor in the design of deep geological repositories.

In the past decades, pure bentonite or bentonite/sand mixture was widely investigated as a sealing/backfilling material for the easy control of its swelling pressure (Komine and Ogata, 1994, 1999). A number of studies have been conducted on the swelling pressure of different compacted bentonites and their mixture with sand, such as Kunigel-V1 bentonite (Sun et al., 2009), MX80 bentonite (Karnland et al., 2008; Saba et al., 2014), Calcigel bentonite (Agus and Schanz, 2008), Tsukinuno bentonite (Komine and Ogata, 1999) and GMZ bentonite (Ye et al., 2007; Cui et al., 2012; Sun et al., 2015, 2017). The swelling pressure of bentonite/sand mixture has been characterized quantitatively based on the montmorillonite void ratio (Sun et al., 2009; Sun et al., 2015, 2017), dry

density of bentonite (Dixon et al., 1985; Lee et al., 1999; Agus and Schanz, 2008), effective dry density of montmorillonite (Dixon et al., 2002; Powell et al., 2013), and initial degree of saturation of montmorillonite (Rao and Ravi, 2015).

The French National Agency for Nuclear Waste Management (ANDRA) proposed to use a mixture of bentonite and excavated Callovo-Oxfordian (COx) claystone as the sealing/backfilling material. This aims to reduce the excavation waste and to better ensure the compatibility of chemistry with the host rock (Tang et al., 2011; Wang et al., 2012, 2014). Wang et al. (2012) worked on a MX80 bentonite/crushed COx claystone mixture at a proportion of 70/30 in dry mass and found that the unique relationship between the swelling pressure and bentonite dry density could be extended to this mixture, the contribution of claystone to swelling pressure being negligible. However, the swelling mechanism of bentonite/claystone mixtures with bentonite fractions lower than 70% has not been well understood.

In this study, the swelling pressure of MX80 bentonite/crushed COx claystone mixture with different dry densities and bentonite fractions was studied. The role of claystone in the development of swelling pressure of the mixture was analyzed, allowing an inhibition factor to be defined for describing the effect of bentonite on the swelling of claystone. A novel method was then proposed to predict the swelling pressure of bentonite/claystone mixture in the full range of bentonite fraction.

2 Materials and experimental methods

2.1 Materials

The commercial MX80 bentonite tested in this study was extracted from Wyoming, USA. Table 1 summarizes the basic physical and chemical properties of MX80 bentonite. The maximum grain size of the bentonite powder is 2 mm and the clay-size fraction (< 2 μm) represents 84%. The density of

bentonite grains was measured to be 2.00 Mg/m^3 by immersing clay powders into a non-aromatic hydrocarbon fluid (Kerdane) using a pycnometer. The initial suction measured by hygrometer WP4 was 101 MPa.

The COx claystone was extracted at around 490 m depth from the Underground Research Laboratory (URL) at Bure, France. The claystone contains 40-45% clay minerals (mainly interstratified illite-smectite), 30% carbonates and 2-30% quartz and feldspar, with a specific gravity of 2.70 (Fouché et al., 2004). It was crushed into fine powders with grain size less than 2.0 mm. More than 30% grains were smaller than 2 μm. The density of the claystone grains is 2.31 Mg/m^3. The initial suction measured by hygrometer WP4 was 27 MPa.

In this study, a synthetic water (see Table 2 for the receipt of preparation), which has the same chemical composition as the site groundwater from the URL in Bure, was used for hydration. The total mass of dissolved solids is 4.545 g/L, which corresponds to a salinity (ratio of salt mass to solution mass) lower than 0.5%.

2.2 Sample preparation

A series of tests were conducted on compacted claystone and MX80 bentonite/claystone mixtures with bentonite fractions of 10, 20, 30, 50, and 70% in dry mass. The bentonite and claystone, with initial water contents of 11.4% and 6.1%, respectively, were mixed for more than 10 min to reach a homogeneous state. Subsequently, samples were statically compacted in a cylindrical mold at a constant displacement rate of 0.05 mm/min to reach the target dry density (Table 3). This rate was chosen to ensure zero air over pressure in soil during compaction. After decompression, the samples had a diameter of 50 mm and a height of 10 mm.

2.3 Experimental methods

Twenty-five swelling pressure tests were carried out using a constant-volume cell at a temperature of 20±1°C. The details about the constant-volume cell can be found in Saba et al. (2014). The compacted samples were pushed into the testing cell from the mold and placed between two porous stones and filter papers. The top cap was locked by a screw. The samples were hydrated from bottom through the water inlet connected to the synthetic water reservoir. The swelling pressure was monitored by a force transducer mounted below the test cell and all data were collected by a data logger. The maximum deformations of the apparatus and filter papers in this study were estimated to be 0.0049 and 0.0169 mm, corresponding to a small reduction of 2.3% in maximum swelling pressure. Thus, the volume change of samples throughout the water-uptake process was ignored.

3 Experimental results

3.1 Swelling pressure kinetics

The evolution of swelling pressure for samples with different bentonite fractions and dry densities is presented in Fig. 1. On the whole, for the samples with high bentonite fractions (larger than 50%) and high dry densities (larger than 1.50 Mg/m^3), the swelling pressure increased rapidly and then reached stabilization. For the samples with low bentonite fractions (smaller than 20%) and low dry densities (smaller than 1.78 Mg/m^3), the swelling pressure started with a fast increase followed by a peak value, a decrease and then reached stabilization. The presence of these peaks is related to the collapse of macro-pores between soil grains (Pusch, 1982; Komine and Ogata, 1994). The lower the dry density, the larger the volume of the macro-pores among grains (Lloret and Villar, 2007). At the same dry density, more macro-pores are expected in the samples with larger fractions of claystone, because of the higher unit mass of claystone (2.31 Mg/m^3) as compared with that of bentonite (2.00 Mg/m^3). It can also be observed that the time required to reach stabilization decreased with the

decrease of dry density and bentonite fraction, which can be explained by the higher hydraulic conductivity of samples with a lower dry density and a larger claystone fraction.

3.2 Relationship between final swelling pressure and dry density of the mixture

Fig. 2 depicts the changes of final swelling pressure (P_s) with the dry density of samples. The results of Karnland et al. (2008) on pure MX80 bentonite, Tang et al. (2011) on pure COx claystone, Wang et al. (2012) and Zhang and Kröhn (2019) on MX80 bentonite/COx claystone mixture are also presented. The swelling pressure values remarkably agree even though the tested materials were from different batches, suggesting that the influence of MX80 bentonite and claystone batches was not enough as to be relevant in the swelling pressure tests. For a given bentonite fraction, the final swelling pressure increased with increasing dry density. At the same dry density, the final swelling pressure of bentonite/claystone mixture after saturation was much lower than that of pure bentonite, indicating that the addition of claystone reduced the global swelling capability.

4 Interpretation and discussion

4.1 Contribution of claystone to swelling pressure

As shown in Fig. 3a, each bentonite-based mixture after the full bentonite hydration process can be divided into four parts: bentonite, voids in bentonite, additive (crushed COx claystone or sand) and voids in additive (Wang et al., 2012; Deng et al., 2017). The bentonite dry density (ρ_{db}) can be formulated by the following equation:

$$\rho_{db}=\frac{(B/100)\rho_m G_{sa}\rho_w}{G_{sa}\rho_w(1+w_m/100)-\rho_m(1-B/100)(1+G_{sa}w_a)}=\frac{(B/100)\rho_{dm} G_{sa}\rho_w}{G_{sa}\rho_w-\rho_{dm}(1-B/100)(1+G_{sa}w_a)} \quad (1)$$

where ρ_m (Mg/m^3) is the mixture density; ρ_{dm} (Mg/m^3) is the dry density of the mixture; ρ_w is the water unit mass; B (%) is the bentonite fraction (in dry mass) in the mixture; w_m is the water content of the mixture; w_a is the water content of additive; G_{sa} is the specific gravity of additive.

For bentonite/sand mixtures, the water content of inactive sand is regarded as zero and the bentonite dry density can be calculated directly using Eq. (1). A unique relationship has been identified between swelling pressure and dry density of Avonseal (Gray et al., 1984), Calcigel (Agus and Schanz, 2008), GMZ (Cui et al., 2012) and MX80 (Saba, 2013) bentonites regardless of the bentonite fraction. For the MX80 bentonite/claystone mixture, the bentonite dry density of samples cannot be calculated directly since the water content of claystone after saturation is unknown. In terms of swelling pressure, the swelling capacity of pure bentonite is more than 100 times larger than that of pure claystone at the same dry density (Fig. 3b) and the initial suction of pure bentonite is about 4 times higher than that of pure claystone. During wetting, the bentonite in the mixture swelled rapidly and came in full contact with the claystone while the volume change of the claystone was influenced by the swelling pressure from bentonite. To determine the bentonite and claystone dry densities, the final pressure at the interface of bentonite and claystone grains was assumed to be equal to the global swelling pressure. This assumption was also adopted by Yang et al. (2002) when investigating the consolidation behavior of lumpy granular soil under one-dimensional condition. In this case, the bentonite dry density in the mixture can be estimated according to the relationship between the swelling pressure of pure bentonite and its dry density (Fig. 3b):

$$P_s=1.652\times10^{-4}\exp^{6.781\rho_{db}} \quad (2)$$

At a certain global swelling pressure P_s, the corresponding bentonite dry density ρ_{db} in the bentonite/claystone mixture can be back-calculated through the unique relationship for pure bentonite. The claystone dry density ρ_{dc} in the mixture, the ratio of solid mass of claystone to the volume occupied by claystone (Fig. 3a), can be calculated using Eq. (3):

$$\rho_{dc}=\frac{m_{sc}}{V\text{-}V_b}=\frac{V\rho_{dm}(1\text{-}B/100)}{V\text{-}\frac{V\rho_{dm}(B/100)}{\rho_{db}}}=\frac{\rho_{db}\rho_{dm}(1\text{-}B/100)}{\rho_{db}\text{-}\rho_{dm}(B/100)} \quad (3)$$

where m_{sc} is the solid mass of claystone; V is the total volume of the mixture; V_b is the volume of bentonite.

Then, the claystone void ratio e_c in the mixture can be deduced using Eq. (4):

$$e_c=\frac{G_{sc}\rho_w}{\rho_{dc}}\text{-}1 \quad (4)$$

where G_{sc} is the specific gravity of claystone. The calculated e_c is summarized in Table 3.

If the claystone can swell without the influence of bentonite, the expected claystone dry density ρ_{dc}^{e} needed to achieve the above swelling pressure P_s can be similarly obtained from the correlation between the swelling pressure of pure claystone and its dry density (Fig. 3b): :

$$P_s=2.208\times10^{-8}\exp^{8.802\rho_{dc}^{e}} \quad (5)$$

Correspondingly, the expected claystone void ratio e_c^e can be deduced using Eq. (6):

$$e_c^e=\frac{G_{sc}\rho_w}{\rho_{dc}^{e}}\text{-}1 \quad (6)$$

During wetting, the stress states of claystone grains in bentonite/claystone mixture and pure claystone are different. In the former, the wetting of claystone is under the pressure imposed by the swelling of bentonite and the water absorption of claystone is restrained (Attom and Barakat, 2000). By contrast, in the latter, the pressure between claystone grains gradually increases with wetting. Therefore, at a given global swelling pressure, e_c in the bentonite/claystone mixture should be smaller than e_c^e, which is corroborated by the calculated result in Table 3. The difference between e_c and e_c^e physically represents the inhibition degree of bentonite on the swelling of claystone. On the whole, the larger the bentonite fraction, the larger the difference and the greater the inhibition effect.

For further analysis of the interaction between bentonite and claystone in swelling pressure

development, an inhibition factor η is defined as follows:

$$\eta=\frac{e_c^e-e_c}{e_c^e}=1-\frac{e_c}{e_c^e} \quad (7)$$

The calculated inhibition factor values for the samples tested are summarized in Table 3. Fig. 4a depicts the variation of η with bentonite fraction. For pure bentonite, the value of inhibition factor is 1; for pure claystone, it equals 0. The inhibition factor increases with the increasing bentonite fraction, following a nonlinear relationship. This relationship can be well described by the following expression with a squared correlation coefficient $R^2 = 0.972$:

$$\eta=\frac{1}{1+e^{10.664(0.595-B/100)}} \quad (8)$$

From Fig. 4a, two inflection points of the sigmoidal curve can be identified, at approximately 40% and 70% bentonite fractions. The inhibition effect of bentonite on the swelling of claystone can be divided into three zones according to these two critical values, that is, Zone I, $100 \geqslant B \geqslant 70$; Zone II, $70 > B \geqslant 40$; Zone III, $40 > B \geqslant 0$. Fig. 4b shows the sketch of bentonite/claystone mixture before and after full saturation in the three zones.

In Zone I, $100 \geqslant B \geqslant 70$, the inhibition factor η is larger than 0.73. The fully swollen bentonite grains form a matrix and claystone grains disperse into the matrix. The claystone grains behave as an inert material and their swelling is almost completely inhibited by bentonite. After wetting, the claystone void ratio e_c in the mixture (Table 3) is even slightly less than the initial void ratio of claystone grain (0.17), due to the collapse of claystone under the swelling pressure induced by bentonite.

In Zone II, $70 > B \geqslant 40$, the inhibition factor η is between 0.11 and 0.73. The swelling of claystone grains is partially restrained by bentonite and the claystone can swell in volume and fill up some voids in the mixture. In this case, partially swelling of the claystone will contribute to the

210 global swelling pressure.

211 In Zone III, $40>B\geqslant 0$, the inhibition factor η is smaller than 0.11. Both claystone and bentonite
212 grains swell upon wetting. The fully swollen bentonite grains disperse in the skeleton formed by the
213 swollen claystone. The claystone void ratio e_c in the mixture is very close to the expected claystone
214 void ratio e_c^e, suggesting that the global swelling pressure is governed by claystone.

215 *4.2 Estimation of swelling pressure of bentonite/claystone mixture*

216 According to the inhibition factor determined above and the relationships between swelling pressure
217 and dry density for pure bentonite and claystone, the swelling pressure of samples with different
218 bentonite fractions and dry densities can be computed following an iteration procedure. Fig. 5 is a
219 flowchart showing how to predict the swelling pressure of MX80 bentonite/COx claystone mixture
220 in the full range of bentonite fraction. The general outline of this procedure is summarized as follows:
221 (a) to assign an initial value of swelling pressure P_0;
222 (b) to back-calculate the expected claystone dry density based on Eq. (5) and to determine the
223 corresponding expected claystone void ratio using Eq. (6);
224 (c) to determine the inhibition factor using Eq. (8) and to compute the claystone void ratio in the
225 bentonite/claystone mixture using Eq. (7);
226 (d) to apply Eq. (4) to calculate the claystone dry density and to back-calculate the bentonite dry
227 density using Eq. (3);
228 (e) to compute the swelling pressure P_1 according to Eq. (2);
229 (f) to judge the absolute error between P_1 and P_0: if $|P_1-P_0|$ is smaller than a certain tolerance α
230 (0.0001 MPa in this study), P_1 is the predicted value of swelling pressure; else, to assign $P_0 = P_1$ and
231 to go to step (a) for a new iteration.

The predicted and the measured swelling pressures are compared in Fig. 2, as a function of the dry density of the mixture, showing a good agreement. This agreement shows the performance of the proposed method as well as the relevance of the identified swelling mechanism.

5 Conclusions

The swelling pressure of MX80 bentonite/COx claystone mixture with different bentonite fractions was investigated by carrying out constant-volume swelling pressure tests. The obtained results allow the following conclusions to be drawn:

The swelling of claystone in the mixture can be inhibited by bentonite and the contribution of claystone to the global swelling pressure depends on the bentonite fraction (B). An inhibition factor was introduced as a function of the bentonite fraction to describe the inhibition effect. According to two inflection points (40% and 70%), the inhibition effect can be divided into three zones (Zone I, $100 \geqslant B > 70$; Zone II, $70 \geqslant B > 40$; Zone III, $40 \geqslant B \geqslant 0$). In Zone I, the swelling of claystone is almost totally inhibited by bentonite; in Zone II, the swelling of claystone grains is partially restrained by bentonite and the claystone can swell and contribute to the global swelling pressure of the mixture; in Zone III, claystone fully swells upon wetting and the claystone governs the global swelling pressure.

A predictive method was proposed, allowing the swelling pressure of the mixture with different bentonite fractions and dry densities to be calculated. The good agreement between the calculated and measured swelling pressure values showed the performance of the proposed method as well as the relevance of the identified swelling mechanism.

Acknowledgments

The authors thank the China Scholarship Council (CSC). The support provided by the French National Agency for Nuclear Waste Management (ANDRA) is also greatly acknowledged.

References

Agus, S.S., Schanz, T., 2008. A method for predicting the swelling pressure of compacted bentonites. Acta Geotech. 3(2), 125.

Attom, M.F., Barakat, S., 2000. Investigation of three methods for evaluating swelling pressure of soils. Environ. Eng. Geosci. 6(3), 293-299.

Bian, X., Cui, Y.J., Li, X.Z., 2018. Voids effect on the swelling behaviour of compacted bentonite. Géotechnique, 1-13.

Cui, S.L., Zhang, H.Y., Zhang, M., 2012. Swelling characteristics of compacted GMZ bentonite–sand mixtures as a buffer/backfill material in China. Eng. Geol. 141, 65-73.

Deng, Y.F., Wu, Z.L., Cui, Y.J., Liu, S.Y., Wang, Q., 2017. Sand fraction effect on hydro-mechanical behavior of sand-clay mixture. Appl. Clay Sci. 135, 355-361.

Dixon, D.A., Gray, M.N., Thomas, A.W., 1985. A study of the compaction properties of potential clays and buffer mixtures for use in nuclear fuel waste disposal. Eng. Geol. 21(3/4):247-255.

Dixon, D.A., Chandler, N.A., Baumgartner, P., 2002. The influence of groundwater salinity and influences on the performance of potential backfill materials. Proceedings of the 6th International Workshop on Design and Construction of Final Reposito- ries, Backfilling in Radioactive Waste Disposal, Brussels, Belgium, 11–13 March 2002. ONDRAF/NIRAS, Brussels, Belgium (Transactions, Session IV, paper 9).

Gray, M.N., Cheung, S.C.H., Dixon, D.A., 1984. Swelling pressures of compacted bentonite/sand mixtures. Mat. Res. Soc. Symp, 44, 523-530.

Fouché, O., Wright, H., Le Cléac'h, J.M., Pellenard, P., 2004. Fabric control on strain and rupture of heterogeneous shale samples by using a non-conventional mechanical test. Appl. Clay Sci.

26(1-4), 367-387.

Karnland, O., Nilsson, U., Weber, H., Wersin, P., 2008. Sealing ability of Wyoming bentonite pellets foreseen as buffer material–laboratory results. Phys. Chem. Earth Parts A/B/C, 33, S472-S475.

Komine, H., Ogata, N., 1994. Experimental study on swelling characteristics of compacted bentonite. Can. Geotech. J. 31(4), 478-490.

Komine, H., Ogata, N., 1999. Experimental study on swelling characteristics of sand-bentonite mixture for nuclear waste disposal. Soils Found. 39(2), 83-97.

Lee, J.O., Cho, W.J., Chun, K.S., 1999. Swelling pressures of a potential buffer material for high-level waste repository. J. Korean Nucl. Soc. 31(2), 139-150.

Lloret, A., Villar, M.V., 2007. Advances on the knowledge of the thermo-hydro-mechanical behaviour of heavily compacted "FEBEX" bentonite. Phys. Chem. Earth Parts A/B/C 32(8-14), 701-715.

Powell, J.S., Siemens, G.A., Take, W.A., Remenda, V.H., 2013. Characterizing the swelling potential of Bearpaw clayshale. Eng. Geol. 158, 89-97.

Pusch, R., 1982. Mineral–water interactions and their influence on the physical behavior of highly compacted Na bentonite. Can. Geotech. J. 19(3), 381-387.

Rao, S.M., Ravi, K., 2015. Influence of initial degree of saturation on swell pressures of compacted Barmer bentonite specimens. Ann. Nucl. Eng. 80, 303-311.

Saba, S., 2013. Hydro-mechanical behaviour of bentonite-sand mixture used as sealing materials in radioactive waste disposal galleries (Doctoral dissertation, Université Paris-Est).

Saba, S., Barnichon, J. D., Cui, Y. J., Tang, A. M., Delage, P., 2014. Microstructure and anisotropic swelling behaviour of compacted bentonite/sand mixture. J. Rock Mech. Geotech. Eng. 6(2),

126-132.

Sellin, P., Leupin, O.X., 2013. The use of clay as an engineered barrier in radioactive-waste management–a review. Clays Clay Miner. 61(6), 477-498.

Sun, D.A., Cui, H., Sun, W.J., 2009. Swelling of compacted sand-bentonite mixtures. Appl. Clay Sci. 43(3-4), 485-492.

Sun, W.J., Wei, Z.F., Sun, Da., Liu, S.Q., Fatahi, B., Wang, X.Q., 2015. Evaluation of the swelling characteristics of bentonite-sand mixtures. Eng. Geol. 199, 1-11.

Sun, W.J., Zong, F.Y., Sun, D.A., Wei, Z.F., Schanz, T., Fatahi, B., 2017. Swelling prediction of bentonite-sand mixtures in the full range of sand content. Eng. Geol. 222, 146-155.

Tang, A.M., Cui, Y.J., Le, T.T., 2008. A study on the thermal conductivity of compacted bentonites. Appl. Clay Sci. 41 (3-4), 181–189.

Tang, C.S., Tang, A.M., Cui, Y.J., Delage, P., Schroeder, C., De Laure, E., 2011. Investigating the pressure of compacted crushed-Callovo-Oxfordian claystone. Phys. Chem. Earth Parts A/B/C 36 (17-18), 1857-1866.

Villar, M.V., Lloret, A., 2008. Influence of dry density and water content on the swelling of a compacted bentonite. Appl. Clay Sci. 39(1-2), 38-49.

Wang, Q., Tang, A.M., Cui, Y.J., Delage, P., Gatmiri, B., 2012. Experimental study on the swelling behaviour of bentonite/claystone mixture. Eng. Geol. 124, 59-66.

Wang, Q., Cui, Y.J., Tang, A.M., Delage, P., Gatmiri, B., Ye, W.M., 2014. Long-term effect of water chemistry on the swelling pressure of a bentonite-based material. Appl. Clay Sci. 87, 157-162.

Yang, L.A., Tan, T.S., Tan, S.A., Leung, C.F., 2002. One-dimensional self-weight consolidation of a lumpy clay fill. Géotechnique 52(10), 713-725.

320 Ye, W.M., Schanz, T., Qian, L.X., Wang, J., Arifin, Y., 2007. Characteristics of swelling pressure of
321 densely compacted Gaomiaozi bentonite GMZ01. Chin. J. Rock Mech. Eng. 26 (S2), 3861–
322 3865 (in Chinese).
323 Zhang, C.L., Kröhn, K.P., 2019. Sealing behaviour of crushed claystone–bentonite mixtures.
324 Geomech. Energy Environ. 17, 90-105.
325

List of Tables

List of Figures

344 **Table 1** Physical and chemical properties of MX80 bentonite (data from Tang et al. (2008), Saba (2013) and Wang et al. (2014))

Soil property	Description
Specific gravity	2.76-2.77
Consistency limit	
Liquid limit (%)	520-575
Plastic limit (%)	42-53
Plasticity index (%)	478-522
Cation exchange capacity (CEC) (meq/100 g)	78-85
Main exchangeable cations (meq/100 g)	
Na^+	60-67
K^+	1
Mg^{2+}	3-4
Ca^{2+}	5-8
Main minerals	
Montmorillonite (%)	70-92
Quartz (%)	3-15

345

346 **Table 2** Receipt for preparing the synthetic water

Components	NaCl	$NaHCO_3$	KCl	$CaSO_4 \cdot 2H_2O$	$MgSO_4 \cdot 7H_20$	$CaCl_2 \cdot 2H_2O$	Na_2SO_4	Total
Content (g/L)	1.950	0.130	0.035	0.630	1.020	0.080	0.700	4.545

347

348 **Table 3** Test program and main results

Test No.	Bentonite fraction B (%)	Dry density of sample ρ_{dm} (Mg/m^3)	Initial water content w_m (%)	Bentonite dry density ρ_{db} (Mg/m^3)	Claystone void ratio e_c	Expected claystone void ratio e_c^e	Inhibition factor η	Final swelling pressure P_s (MPa)
01	70	1.38	9.8	1.15	0.08	0.42	0.81	0.43
02	70	1.50	9.8	1.29	0.13	0.34	0.60	1.11
03	70	1.63	9.8	1.42	0.07	0.28	0.74	2.53
04	70	1.71	9.8	1.48	0.02	0.25	0.91	3.94
05	50	1.27	8.8	0.98	0.49	0.52	0.06	0.13
06	50	1.56	8.8	1.26	0.30	0.36	0.16	0.85
07	50	1.73	8.8	1.39	0.18	0.29	0.38	2.10
08	50	1.76	8.8	1.44	0.19	0.27	0.28	2.91
09	30	1.50	7.7	1.06	0.47	0.47	0.00	0.22
10	30	1.60	7.7	1.16	0.41	0.41	0.00	0.46
11	30	1.68	7.7	1.24	0.36	0.37	0.02	0.78
12	30	1.79	7.7	1.35	0.30	0.31	0.06	1.59
13	30	1.89	7.7	1.43	0.23	0.28	0.18	2.72
14	30	1.99	7.7	1.52	0.18	0.23	0.23	5.23
15	20	1.60	7.2	1.08	0.49	0.46	-0.06	0.26
16	20	1.69	7.2	1.16	0.41	0.41	0.01	0.44
17	20	1.77	7.2	1.23	0.35	0.38	0.06	0.70
18	20	1.88	7.2	1.38	0.31	0.30	-0.02	1.93
19	10	1.61	6.6	0.98	0.56	0.52	-0.08	0.14
20	10	1.68	6.6	1.06	0.50	0.47	-0.07	0.23
21	10	1.78	6.6	1.14	0.42	0.42	0.01	0.39
22	10	1.90	6.6	1.29	0.35	0.34	-0.02	1.07
23	0	1.80	6.1	-	-	-	0	0.15
24	0	1.90	6.1	-	-	-	0	0.47
25	0	1.99	6.1	-	-	-	0	0.79

349

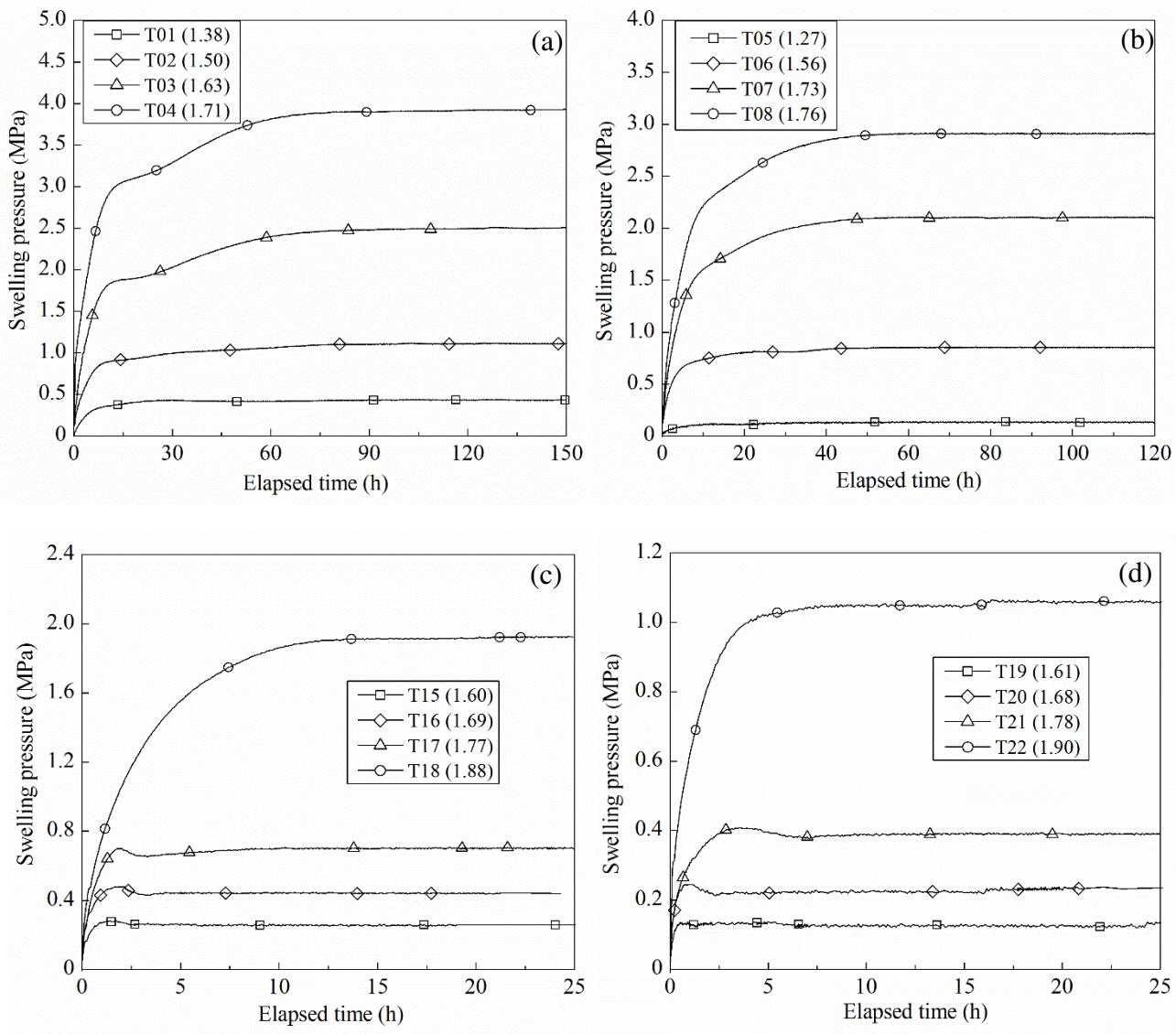

Fig. 1. Evolution of swelling pressure of bentonite/claystone mixture with bentonite fractions of (a) 70%; (b) 50%; (c) 20%; (d) 10%

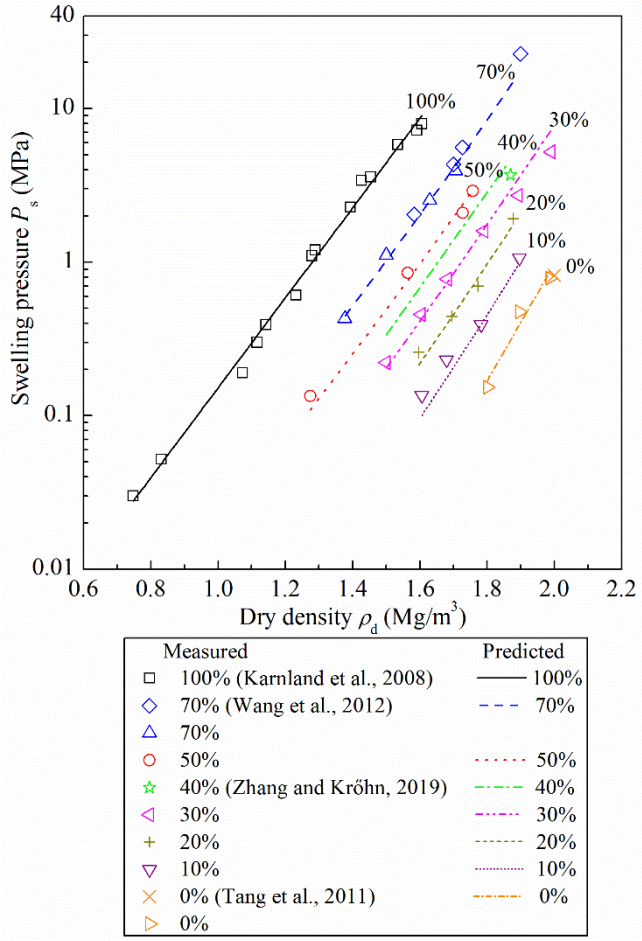

353
354 **Fig. 2.** Measured and predicted swelling pressures as function of the dry density of samples. Note: the legend indicates the bentonite
355 fraction

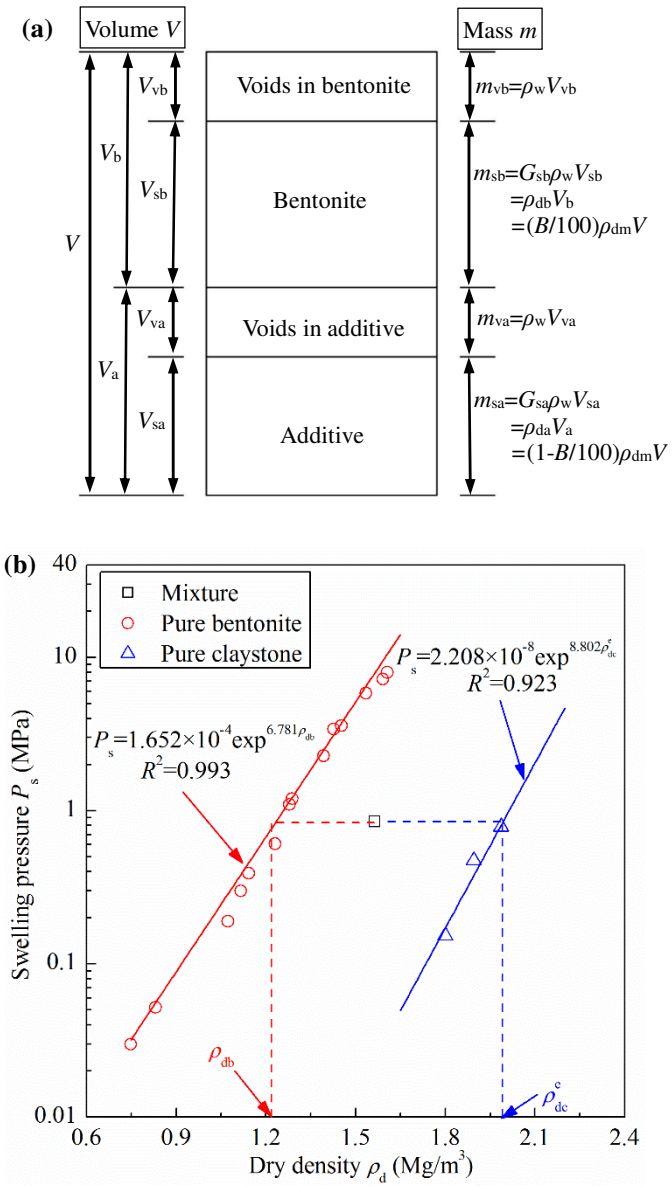

Fig. 3. Composition of bentonite/additive mixture (a) and calculation of bentonite dry density and expected claystone dry density of bentonite/claystone mixture (b)

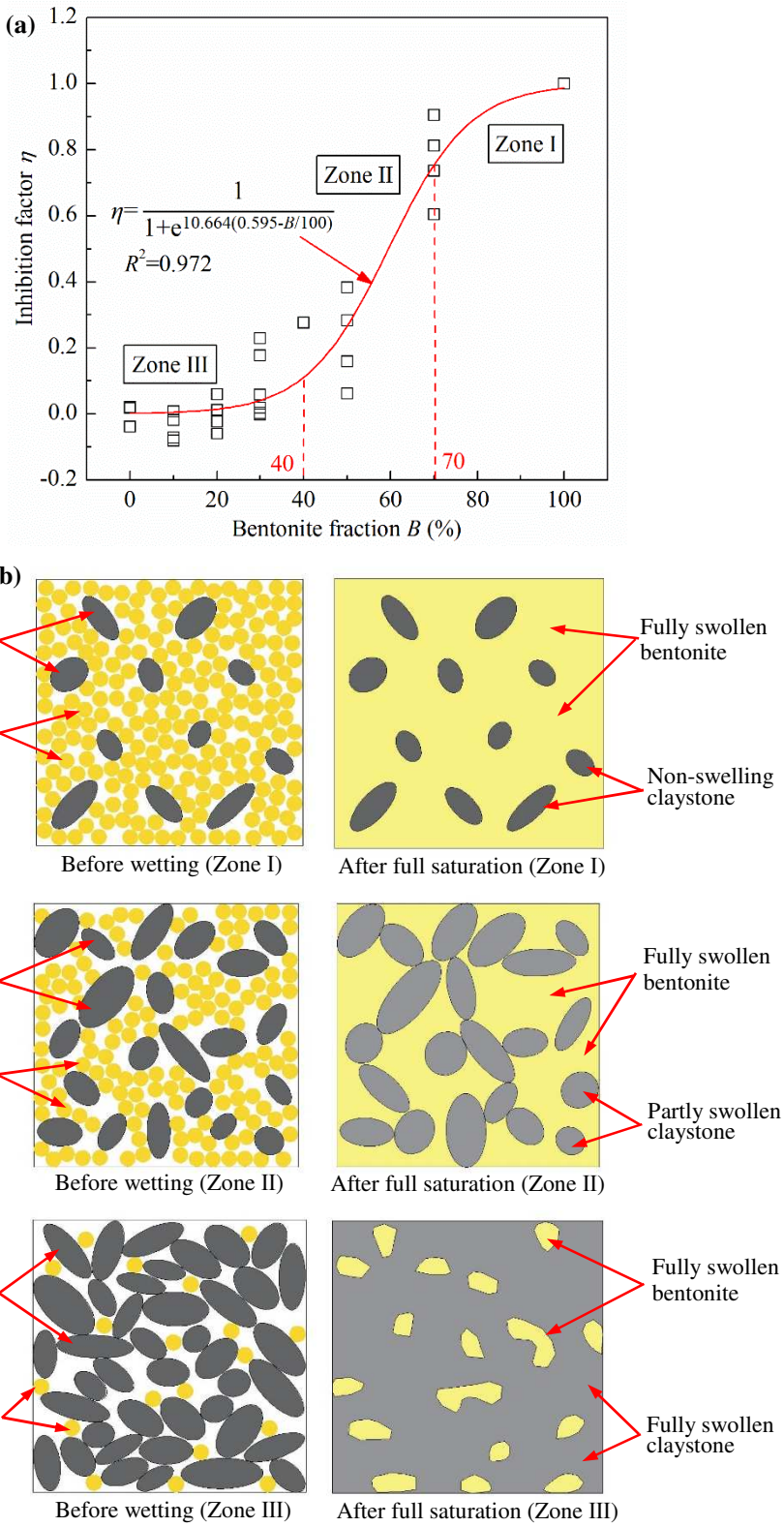

Fig. 4. Evolution of inhibition factor with bentonite fraction (a) and swelling mechanism of bentonite/claystone mixture in three zones (b). Note: the zones for bentonite and claystone after full saturation include voids in them

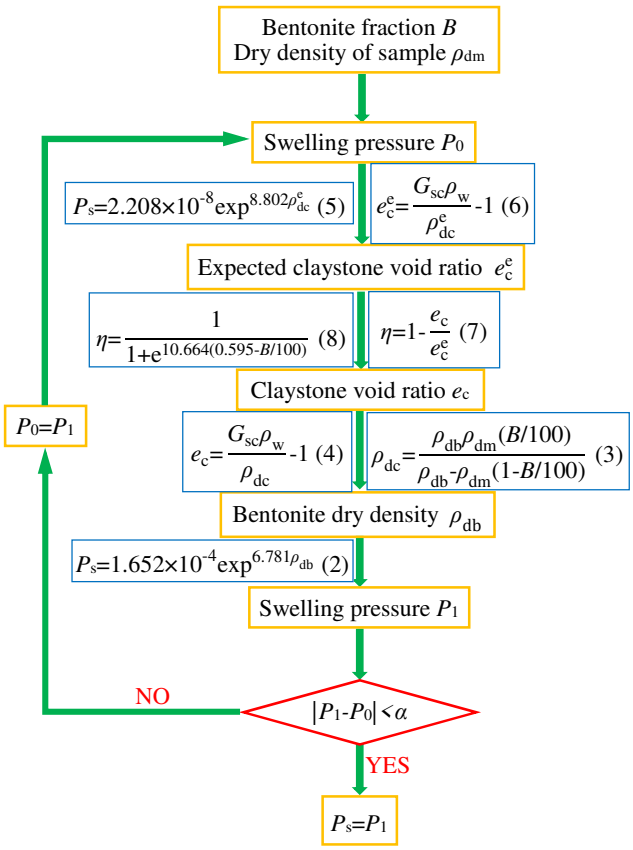

Fig. 5. Flowchart for swelling pressure prediction for bentonite/claystone mixture in the full range of bentonite fraction